Published in final edited form as:
Dev Cell. 2013 April 29; 25(2): 132–143. doi:10.1016/j.devcel.2013.03.003.

CASZ1 Promotes Vascular Assembly and Morphogenesis Through the Direct Regulation of an EGFL7/RhoA-mediated pathway

Marta S. Charpentier[1,3,#], **Kathleen S. Christine**[1,2,#], **Nirav M. Amin**[1,3], **Kerry M. Dorr**[1,3], **Erich J. Kushner**[2], **Victoria L. Bautch**[1,2,3,5], **Joan M. Taylor**[1,4], and **Frank L. Conlon**[1,2,3,5,*]

[1]McAllister Heart Institute, University of North Carolina at Chapel Hill, Chapel Hill, NC 27599-3280, USA

[2]Department of Biology, University of North Carolina at Chapel Hill, Chapel Hill, NC 27599-3280, USA

[3]Department of Genetics, University of North Carolina at Chapel Hill, Chapel Hill, NC 27599-3280, USA

[4]Departments of Pathology and Laboratory Medicine, University of North Carolina at Chapel Hill, Chapel Hill, NC 27599-3280, USA

[5]Lineberger Comprehensive Cancer Center, University of North Carolina at Chapel Hill, Chapel Hill, NC 27599-3280, USA

Summary

The formation of the vascular system is essential for embryonic development and homeostasis. However, transcriptional control of this process is not fully understood. Here we report an evolutionarily conserved role for the transcription factor CASZ1 in blood vessel assembly and morphogenesis. In the absence of CASZ1, *Xenopus* embryos fail to develop a branched and lumenized vascular system, and CASZ1-depleted human endothelial cells display dramatic alterations in adhesion, morphology, and sprouting. Mechanistically, we show CASZ1 directly regulates *Epidermal Growth Factor-Like Domain 7* (*Egfl7*). We further demonstrate that defects of CASZ1 or EGFL7-depleted cells are in part due to diminished RhoA expression and impaired focal adhesion localization. Moreover, these abnormal endothelial cell behaviors in CASZ1-depleted cells can be rescued by restoration of *Egfl7*. Collectively, these studies show CASZ1 is required to directly regulate a unique EGFL7/RhoA-mediated pathway to promote vertebrate vascular development.

Introduction

Endothelial cells (ECs) are building blocks for the formation of a functional vascular system during embryonic development. Early stages of blood vessel development occur via vasculogenesis whereby mesodermal cells differentiate into EC progenitors that

*Correspondence: frank_conlon@med.unc.edu.
#These authors contributed equally to this work.

subsequently proliferate, migrate, and assemble into vascular cords. Cords then undergo tubulogenesis, or lumen formation, continuing to mature by angiogenesis where vessels sprout, branch, and remodel. Vessels then become surrounded and stabilized by pericytes and smooth muscle cells that provide structural support (De Val, 2011; Patan, 2000). The critical nature of these events is emphasized by observations that disruption of these processes is associated with human disease states including cancer, stroke, and atherosclerosis, therefore necessitating a better understanding of transcriptional networks that regulate these key developmental steps (Carmeliet, 2003; Carmeliet and Jain, 2011; Potente et al., 2011).

While numerous transcription factors have been discovered to regulate endothelial gene expression, relatively few factors are necessary for development. Deletions or mutations of a number of single genes, especially members of Ets and forkhead families, result in moderate to no vascular phenotypes likely due to functional redundancy (Barton et al., 1998; De Val, 2011; De Val and Black, 2009; Lelievre et al., 2001). Previous studies have implicated the zinc finger transcription factor CASZ1 in cardiovascular development with depletion of CASZ1 in *Xenopus* embryos resulting in failure of a subset of progenitor cells to differentiate into cardiomyocytes (Christine and Conlon, 2008). Recent genome-wide association studies have shown a genetic link between human *Casz1* and high blood pressure and hypertension, suggesting a possible role for CASZ1 in EC biology (Levy et al., 2009; Takeuchi et al., 2010). However, no studies have addressed expression, function, or transcriptional targets of CASZ1 in vascular tissue.

Despite an essential role for the vasculature in development and disease, our knowledge of molecular mechanisms controlling these events remains incomplete (De Val and Black, 2009). One protein recently shown to play a role in EC morphogenesis is *Epidermal Growth Factor-Like Domain 7* (*Egfl7*), an extracellular matrix (ECM) protein expressed exclusively in EC progenitors and vessels during embryonic and neonatal development. EGFL7 is also expressed in highly vascularized adult organs and is upregulated upon injury (Campagnolo et al., 2005; Fitch et al., 2004; Parker et al., 2004). Depletion studies in zebrafish have defined a role for EGFL7 in tubulogenesis likely through modulation of cell-matrix interactions (Nikolic et al., 2010; Parker et al., 2004). In addition, overexpression of *Egfl7* in mouse results in abnormal patterning of embryonic and postnatal vasculature (Nichol et al., 2010). However, the specific function of EGFL7 has been complicated by recent discovery of microRNA miR-126, the only EC-specific microRNA, within intron 7 of the *Egfl7* locus. While *Egfl7* and miR-126 are co-expressed, the function of miR-126 has indicated a distinct role from its host gene in maintaining vessel integrity and modulating angiogenesis through repression of targets *Spred1* and *PIK3R2* (Fish et al., 2008; Kuhnert et al., 2008; Wang et al., 2008).

In this study, we demonstrate CASZ1 is required for angiogenic sprouting and lumen morphogenesis. CASZ1 regulates EC contractility, adhesion, and sprouting promoting assembly and tubulogenesis of blood vessels. Furthermore, we demonstrate CASZ1 activates *Egfl7*/miR-126 in mammals and *Xenopus* by directly binding to an intronic element but does not regulate miR-126 in *Xenopus*. Moreover, defects associated with CASZ1-depletion can be phenocopied by EGFL7-depletion, and importantly, rescued by restoration of *Egfl7* levels. We further show CASZ1 transcriptional control of EGFL7 modulates EC behavior through RhoA. Collectively, our studies point to a network whereby CASZ1 regulates an EGFL7/RhoA-mediated pathway to promote vessel assembly and morphogenesis.

Results

EC Expression of CASZ1 is Evolutionarily Conserved

Analysis of *Casz1* expression in *Xenopus* embryos showed transcripts in the vitelline vein network (vvn) at a stage when the network is primarily made up of vascular ECs and devoid of smooth muscle cells (Figure 1A)(Christine and Conlon, 2008; Cox et al., 2006; Warkman et al., 2005) suggesting *Casz1* is expressed in vascular ECs. Furthermore, RT-PCR on vascular explants from late tailbud stage embryos (stage 32) demonstrated that *Casz1* is co-expressed in the vitelline vein region with vascular markers, *Msr* and *Erg* (Figure S1A). Consistently, we found CASZ1 co-localizes with the EC-specific marker PECAM in blood vessels of mouse embryos (Figure 1B). We have also cloned human *Casz1* and showed, as in *Xenopus* and mouse, *Casz1* is expressed in primary human umbilical vein ECs (HUVEC) (Figures 1C and 1D). These results taken together with sequence homology and synteny of CASZ1 across vertebrates (Christine and Conlon, 2008) demonstrate CASZ1 is an evolutionarily conserved transcription factor expressed in ECs.

CASZ1 is Required for Vascular Patterning and Lumen Morphogenesis

To ascertain the function of CASZ1 in vascular development, we depleted CASZ1 in *Xenopus* embryos using a morpholino-based approach (Christine and Conlon, 2008). Whole-mount *in situ* hybridization using a panel of EC markers such as *Msr* and *Erg* (Baltzinger et al., 1999; Devic, 1996) demonstrated that at stages when ECs begin to migrate dorsally from ventral blood islands within the trunk region, there were no noticeable differences between control and CASZ1-depleted embryos (stage 29, Figures S1B, S1C, S1J, S1K). However, when ECs begin to assemble into cords (stage 32), defects became apparent whereby CASZ1-depleted embryos displayed a dramatically reduced vascular plexus (Figures 2A-2D, S1D--S1E). Extension of intersomitic vessels from posterior cardinal veins, which is known to occur in *Xenopus* via sprouting angiogenesis in an anterior-to-posterior direction (Cleaver et al., 1997; Levine et al., 2003), was also absent or significantly delayed in CASZ1-depleted embryos (Figures 2A, 2C, 2E, 2G). By mid- to late tadpole stages (stages 36 and 39), vascular networks of CASZ1-depleted embryos were comprised of cords which ran predominately in a dorsal-to-ventral pattern and underwent little to no branching or remodeling (Figures 2E-2H, S1F-S1I, S1L-S1M). Overall, at stage 36, total length of the vitelline vein vasculature and number of branch points and intersomitic vessels were all significantly decreased in CASZ1-depleted embryos implying a role for CASZ1 in sprouting and remodeling of the vasculature (Figure 2I). While our studies focused on vein-derived sprouts, CASZ1-depletion unlikely disrupts arterial/venous differentiation due to proper specification and localization of the aortic arches (arterial) and posterior cardinal veins as well as due to the lack of arterial marker expression in veins (data not shown).

Noting the posterior cardinal veins of CASZ1-depleted embryos appeared thickened (stage 36), we sought to determine the time course of lumen formation in *Xenopus*. At stage 29, control and CASZ1-depleted ECs, as marked by *Msr*, were localized to positions of the future veins but had not yet undergone lumen formation (Figures 2J, 2N). By stage 32, ECs separated in control embryos but remained as aggregates in CASZ1-depleted embryos (Figures 2K, 2O). By stages 36 and 39, the veins of control embryos exhibited well-formed lumens surrounded by *Msr*-positive ECs while CASZ1-depleted veins remained closed and failed to open even at late stages (Figures 2L, 2M, 2P, 2Q). Collectively, these studies demonstrate CASZ1 is required for angiogenic remodeling and lumen morphogenesis during vertebrate vascular development.

Since we have previously established CASZ1 is required for heart development (Christine and Conlon, 2008), we determined if the vascular requirements for CASZ1 were secondary to its role in cardiac tissue. Taking advantage of the amenability of *Xenopus* embryos to organotypic culture (Mandel et al., 2010), we removed anterior regions of embryos, including all cardiac tissue at a stage prior to heart formation. Culture of explants showed in the absence of cardiac tissue, control explants formed vascular networks, as marked by the EC-specific gene *Ami* (Inui and Asashima, 2006), that were indistinguishable from un-manipulated embryos, demonstrating blood flow is not essential for correct patterning of the early vasculature (Figures S1N, S1P). Critically, we observed severe defects in vascular networks of CASZ1-depleted explants, strongly suggesting the role of CASZ1 in vascular development is independent of its role in cardiogenesis (Figures S1O, S1Q).

CASZ1 Regulates EC Behavior

To examine vascular development in more detail and determine if the function of CASZ1 is evolutionarily conserved, we depleted CASZ1 in HUVECs by lentiviral-mediated short hairpin RNA (shRNA, 16-fold decrease in *Casz1* mRNA; Figure 3A). CASZ1-depleted cells displayed a thin and elongated morphology in stark contrast to characteristic cobblestone appearance of uninfected HUVECs or HUVECs infected with control shRNA (Figure 3B).

To determine the precise requirement for CASZ1 and to characterize the dynamics of CASZ1-depleted HUVECs in real time, we coupled time-lapse imaging with quantitative analysis. Time-lapse movies showed that CASZ1-depleted cells initially adhered to plastic or fibronectin-coated substrates but a proportion of cells rounded up and detached (33%, Figure 3C, Movie S1, data not shown). Of CASZ1-depleted HUVECs that adhered, live imaging demonstrated the elongated morphology resulted from defects in contractility whereby the leading edge of CASZ1-depleted cells moved forward without retraction of the trailing edge (Figure 3C, Movie S1). CASZ1-depleted cells also stopped dividing (0% shCasz1 vs. 20% control) and consistently, we failed to detect any phospho-histone H3 (pH3)-positive CASZ1-depleted cells (vs. 3% control cells; Figure S2A). Using fluorescence-activated cell sorting (FACS), we determined CASZ1-depleted ECs were blocked at the G1/S transition as seen by the significantly reduced number of cells in S-phase (Figure S2B). Blockage in G1/S progression was not associated with programmed cell death as determined by cleaved caspase-3 staining (Figure S2C). Furthermore, inability of CASZ1-depleted cells to maintain adhesion to the substrate was not a secondary consequence of cell cycle arrest as wildtype HUVECs chemically treated with mitomycin C did not divide yet remained attached (data not shown). Taken together, these results indicate CASZ1 has a conserved role in vascular development and is required for EC adhesion, contractility, and G1/S cell cycle progression.

To assess how adhesive and morphological defects of CASZ1-depleted cells manifested themselves in vessel assembly, we assessed sprouting using a sprouting angiogenesis assay in which HUVEC-coated beads were placed in fibrin. While control cells displayed elongated sprouts with multiple branch points, similar to our findings in *Xenopus*, CASZ1-depleted HUVECs had strikingly few sprouts and branches (Figure 3D). Live time-lapse imaging further showed that CASZ1-depleted cells extended out from beads to initiate sprout formation but then abruptly detached, indicating that CASZ1 is required for proper EC adhesion to promote angiogenic sprouting (Movie S4).

Isolation of *Egfl7*/miR-126 Locus by CASZ1 Chromatin Immunoprecipitation

To identify direct cardiac and endothelial transcriptional targets of CASZ1, we generated a CASZ1-specific antibody and performed cloning chromatin immunoprecipitation (ChIP) from dissected cardiovascular *Xenopus* tissue (stages 27-29, i.e. same time and tissue

requiring CASZ1)(Figure 4A). We identified 110 putative transcriptional targets including *Egfl7*, an ECM protein specifically secreted by ECs shown to be associated with similar cellular processes as we observe for CASZ1; EC adhesion and vessel tubulogenesis (Figure 4B, Table S1)(Nichol et al., 2010; Nikolic et al., 2010; Parker et al., 2004).

Recently, studies in mouse and zebrafish identified the evolutionarily conserved miR-126 contained within intron 7 of *Egfl7* (Fish et al., 2008; Kuhnert et al., 2008; Wang et al., 2008). We cloned *Egfl7* and miR-126 from *Xenopus* and showed EGFL7 is 47% identical to human and 45% identical to mouse EGFL7, while *Xenopus* miR-126 is completely (100%) conserved between mouse and human (Fitch et al., 2004)(Figure S3A). Genome analysis and characterization of *Xenopus* BACs corresponding to the *Egfl7*/miR-126 locus confirmed that like other model systems, miR-126 is located within intron 7 of the *Xenopus Egfl7* locus (Figure 4B).

Expression analysis revealed *Egfl7* is expressed in all major vessels at all stages of vasculogenesis in *Xenopus*, as reported for zebrafish, mouse, and human (Figures 4C, 4E, 4G, 4I)(Fitch et al., 2004; Parker et al., 2004). Though *Egfl7* and miR-126 have been reported to be co-transcribed and co-expressed in the vasculature, we found *Xenopus* miR-126 has an expression pattern distinct from *Egfl7* as well as that reported in other species (Fish et al., 2008; Wang et al., 2008). Most notably, miR-126 expression is initiated in ECs at stage 32, slightly later than *Egfl7* (stage 29), and we observed strong expression of miR-126, but not *Egfl7*, in the developing somites (Figure S3B-S3I). Taken together these data show that the sequence, genomic arrangement, and vascular expression of *Egfl7* and miR-126 are evolutionarily conserved, however in *Xenopus*, miR-126 has developed additional levels of regulation distinct from *Egfl7*.

Consistent with *Egfl7* being a direct target of CASZ1, analysis in CASZ1-depleted embryos showed *Egfl7* was initiated but not maintained in vascular tissues at all stages analyzed (Figures 4D, 4F, 4H, 4J). Consistently, *Egfl7* levels were significantly reduced in CASZ1-depleted HUVEC (3-fold; Figure 4K). We further observed a dramatic reduction in miR-126 (9-fold) in CASZ1-depleted HUVECs (Figure 4K). These effects were specific as the EC marker *Flk1* was unaltered (Figure 4K). However, we did not observe reduction in miR-126 in CASZ1-depleted *Xenopus* embryos at mid- and late-tadpole stages (stages 32-39, Figures S3E, S3G, S3I). Collectively, these studies demonstrate regulation of *Egfl7* and miR-126 expression in human ECs is dependent on CASZ1 while *Xenopus* miR-126 appears to have evolved a CASZ1-independent mechanism of regulation.

Egfl7 is a Direct Transcriptional Target of CASZ1

To determine whether CASZ1 directly regulates *Egfl7*, we performed *in vivo* transcriptional assays where single copies of intronic regions of *Egfl7* corresponding to the putative CASZ1-bound region (introns 2-5) were placed upstream of a basal promoter driving luciferase activity. Of these intronic regions, only the 5′ half of intron 3 (*E1*) resulted in a dose-dependent, reproducible increase in transcriptional activity in response to CASZ1 (Figures 4L-4M). To determine if CASZ1 endogenously binds to this element *in vivo* and to further refine the region within *E1*, we performed ChIP of endogenous CASZ1 from early embryos (stage 32), a time point when CASZ1 is required for *Egfl7* expression. Results showed CASZ1 binds to nucleotides 59-173 of intron 3 (*E1.2*) but not the most 5′ end of *E1* (*E1.1*)(Figure 4N, data not shown). Thus, CASZ1 directly binds to the *Egfl7* locus *in vivo* and can activate *Egfl7* transcription through a regulatory element within intron 3 of the *Egfl7* locus.

EGFL7 Functions Downstream of CASZ1 to Control Vascular Morphogenesis

To determine if CASZ1 acts through EGFL7 to regulate EC development, we depleted *Egfl7* in embryos using a morpholino that left miR-126 expression intact (Figures S4A-S4E). Strikingly, EGFL7-depletion resulted in vascular phenotypes that phenocopied CASZ1-depletion (Figures 5A-5H, S4F-S4S). As with CASZ1-depleted embryos, we found a reduction in density of ECs within the vitelline vein network (stage 32)(Figures 5A-5D, S4F-S4G, S4J-S4M). Furthermore, while blood vessels did form in EGFL7-depleted embryos, there was significantly reduced branching and intersomitic vessel sprouting at later stages (Figures 5E-5H, S4H-S41, S4N-S4Q). Quantification of vitelline vein networks at stage 36 revealed results similar to CASZ1-depletion whereby the total length of the vasculature and number of branch points and intersomitic vessels of EGFL7-depleted embryos was significantly decreased compared to controls (Figure 5I). Furthermore, like CASZ1-depleted embryos, and in accordance with reports of EGFL7-depletion in zebrafish (Parker et al., 2004), lumens of posterior cardinal veins of EGFL7-depleted embryos failed to form (Figures 5J-5M). Morpholinos targeting the Dicer cleavage site of *Xenopus* pri-miR-126 had no effect on *Egfl7* expression (Figures S5A-S5E) and did not result in gross defects in vessel morphology or patterning, in accordance with reports in zebrafish (Figures S5F-S5U)(Fish et al., 2008). Consistently, lumens of posterior cardinal veins of miR-126-depleted embryos were indistinguishable from controls (Figures S5V-S5Y). Taken together these results imply EGFL7 functions downstream of CASZ1 to regulate angiogenesis and vascular remodeling

Similar to our studies in *Xenopus*, time-lapse imaging of HUVECs revealed depletion of EGFL7 by shRNA (shEgfl7, 11-fold decrease in mRNA; Figure 5N) phenocopied CASZ1-depletion. Most notably, EGFL7-depleted cells demonstrated similar adhesion and proliferation defects as those of CASZ1-depleted cells (Figure 5O, Movie S2) and also displayed an elongated morphology similar to but not as extensive as observed in CASZ1-depleted cells. The sprouting angiogenesis assay further demonstrated similar defects to CASZ1-depleted cells whereby the total length of sprouts and number of branch points were significantly decreased in EGFL7-depleted cells compared to controls (Figure 5P). Live imaging showed failure to sprout was due to the inability of EGFL7-depleted cells to maintain adhesion (Movie S5). Results were specific since we observed minimal effect on expression of *Casz1* or *Flk1* (Figure 5N). Collectively, these studies show *Egfl7* functions downstream of CASZ1 to control vascular morphogenesis in *Xenopus* and humans. In addition, miR-126 does not function downstream of CASZ1 in *Xenopus* vascular development.

Egfl7 and miR-126 Function Downstream of CASZ1 to Regulate Cell Adhesion and Shape

To test if CASZ1 functions through *Egfl7* or miR-126 to regulate vascular development and morphogenesis in human ECs, we assessed if restoration of *Egfl7* or miR-126 levels rescues defects associated with CASZ1-depletion. While 29% of cells infected with shCasz1 rounded up and detached compared to 3% of control cells, infection of CASZ1-depleted cells with adenoviral constructs expressing either human *Egfl7* (Ad-Egfl7) or miR-126 (Ad-miR-126) recovered proper adhesion as only 7.6% and 1% of cells detached, respectively (Figures 6A, S6A-S6B, Movie S3). However, restoration of *Egfl7*, but not miR-126, partially rescued EC morphology associated with CASZ1-depletion as measured by length-to-width ratio (L:W)(Figures 6B, S6C). Restoration of either *Egfl7* or miR-126 failed to rescue proliferation defects (data not shown). Taken together, these studies demonstrate that CASZ1 acts to control EC adhesion through direct transcriptional regulation of *Egfl7* and miR-126. These data further indicate EGFL7 and miR-126 have distinct functions in regards to cell morphology since EGFL7 but not miR-126 can rescue cell shape changes, and further

imply CASZ1 control of G1/S progression occurs by *Egfl7*- and miR-126-independent pathways.

CASZ1 and EGFL7 Regulate RhoA

Past studies have provided evidence that two of the physiological outputs of the CASZ1/EGFL7 pathway, cell adhesion and morphology, are directly controlled by activation of Rho GTPases. Specifically, RhoA is required for actomyosin-dependent cell contractility and formation of focal adhesions (FA)(Burridge and Wennerberg, 2004; Katoh et al., 2011; Parsons et al., 2010). To identify mechanisms that mediate the physiological function of the CASZ1/EGFL7 pathway, we aimed to determine the relationship between CASZ1/EGFL7 and RhoA. We found RhoA activity and levels were dramatically diminished in CASZ1 and EGFL7-depleted cells, however, levels of other Rho proteins such as RhoC were unaltered (Figure 6C, S6D-S6E). The decrease in RhoA protein occurred at the transcriptional level as RhoA but not RhoC mRNA levels were markedly diminished in both CASZ1 and EGFL7-depleted ECs (Figure 6D). However, RhoB levels were slightly increased possibly indicating a compensatory mechanism for loss of RhoA (Figure 6D).

We reasoned reduction of RhoA expression in CASZ1- and EGFL7-depleted cells would result in concomitant impaired downstream activity. Consistently, phosphorylation of regulatory subunit of myosin light chain (p-MLC) was decreased in CASZ1-depleted cells (Figure S6F). To further assess whether decreased RhoA activity directly plays a role in the adhesion and cell shape defects we observe in CASZ1-depleted cells, we analyzed a panel of cytoskeletal and FA markers. Control cells displayed discrete bundles of F-actin stress fibers, as assayed by phalloidin staining, that contained short or punctate bands of FA markers vinculin and phosphorylated paxillin (Figure 6E, left panels). However, CASZ1-depletion mimicked treatment with the Rho kinase (ROCK) inhibitor Y-27632 resulting in diffuse actin networks devoid of stress fibers and failure of vinculin and phosphorylated paxillin to properly localize to adhesion sites on the periphery of the cell (Figure 6E, middle panels)(Narumiya et al., 2000). This phenotype was partially rescued by restoration of *Egfl7* levels in CASZ1-depleted cells (Figure 6E, right panels). Taken together these studies show CASZ1 acts through the direct transcriptional regulation of EGFL7 to control EC adhesion and shape via the RhoA pathway.

Discussion

In this work we demonstrate an essential and conserved role for the CASZ1/EGFL7/RhoA pathway in vascular patterning. Collectively, these data support a mechanism whereby CASZ1 directly binds to and maintains expression of *Egfl7* in ECs. EGFL7 is then localized extracellularly where it modulates signals between ECs and the underlying ECM. This in turn is responsible for transcriptional upregulation and activity of the RhoA GTPase which ultimately mediates EC contractility and adhesive properties to promote assembly, lumen formation, and functionality of the vasculature (Figure 7).

CASZ1 Regulates EC Behavior Via EGFL7/RhoA to Promote Assembly of a Well-Branched Vascular Network

During embryogenesis, ECs assemble into cord-like structures that undergo further remodeling to form the primary vascular plexus. We have shown CASZ1 acts through the direct transcriptional regulation of EGFL7 to promote two critical processes during this period of embryogenesis: sprouting angiogenesis and lumen morphogenesis. The presence of thickened cords lacking lumens in CASZ1-depleted embryos, together with the observation that CASZ1-depleted ECs fail to sprout properly or adhere to extracellular

substrates, strongly implies that CASZ1 functions through the EGFL7/RhoA pathway to maintain proper EC adhesion during vessel assembly.

Casz1 and RhoA

RhoA has been shown to be a central component of pathways which facilitate vascular remodeling. In this regard, RhoA has been demonstrated to be required for stress fiber formation, acting through the actomyosin contractile machinery, and for FA formation (Burridge and Wennerberg, 2004; Chrzanowska-Wodnicka and Burridge, 1996; Katoh et al., 2011; Nobes and Hall, 1995). In accordance with CASZ1 acting through RhoA to promote proper EC adhesion, we find that depleting CASZ1 phenocopies inhibition of RhoA and leads to a lack of discrete stress fibers, decreased myosin II activity, and strikingly, the absence of FA markers at sites of substrate contact. Moreover, these alterations in EC adherence can all be rescued in a CASZ1-depleted background by restoration of *Egfl7*.

The role of RhoA in tubulogenesis has been controversial. While reports have demonstrated RhoA activity is central for lumen formation, for example in the formation of the mouse dorsal aorta (Strilic et al., 2009), other reports have shown that in culture RhoA is not required for lumen formation but rather, for maintenance of patent vessels (Bayless and Davis, 2002). However, the *in vivo* relevance of the latter observation is yet to be determined since the mechanism by which lumens arise in 3D collagen culture differs significantly from that of cord hollowing *in vivo* (Davis et al., 2007; Strilic et al., 2009). Paradoxically, it has been recently demonstrated RhoA and myosin II activity must be suppressed to promote lumen formation of mouse vessels via negative regulation by Ras interacting protein 1 (RASIP1) (Xu et al., 2011). Collectively these studies along with our present findings imply that a precise level of RhoA activity is required for lumen formation with either too low or too high activity leading to failure of vascular cords to hollow and form lumens.

The finding that RhoA protein and mRNA expression are significantly diminished in CASZ1 and EGFL7-depleted HUVECs indicates transcriptional control of RhoA is impaired. Very few studies to date have focused on how RhoA transcription is controlled. While EGFL7 has been shown to interact with lysyl oxidases responsible for vascular elastogenesis as well as some Notch receptors on both ECs and neural stem cells, it is still unclear how these interactions may be influencing RhoA transcription or activity (Lelievre et al., 2008; Nichol et al., 2010; Schmidt et al., 2009). However, our results would support a mechanism by which CASZ1 modulates RhoA signaling through EGFL7 as restoration of *Egfl7* levels in CASZ1-depleted cells rescues adhesion, proper FA marker localization, and stress fiber formation. It was recently shown that RhoA is directly activated by the Myc-Skp2-Miz1-p300 transcriptional complex (Chan et al., 2010). Given a role for c-Myc in embryonic vascular development and later angiogenic remodeling (Baudino et al., 2002; Kokai et al., 2009; Rodrigues et al., 2008), it will be interesting to investigate whether CASZ1 transcriptional regulation of *Egfl7* directly plays into Myc-mediated transcriptional control of RhoA.

Transcriptional Regulation of *Egfl7* and miR-126

Studies on *Egfl7* and miR-126 have identified a 5.4Kb upstream sequence that is sufficient to drive EC-specific expression of a reporter gene in mouse, and mutation of two evolutionarily conserved Ets binding sites within this element eliminated expression in culture (Wang et al., 2008). We have demonstrated CASZ1 is required for expression of *Egfl7* where CASZ1 is endogenously bound to intron 3 of the *Egfl7* locus in developing embryos and depletion of EGFL7 phenocopies CASZ1-depletion in embryos and HUVEC. Consistently, we note CASZ1 is not required for onset of *Egfl7* expression in embryos but

rather its maintenance. Based on our studies, we favor a model by which Ets factors activate *Egfl7* via an upstream element and CASZ1 binds to intron 3 and functions to maintain *Egfl7* levels. This model is complementary to findings for the role of Ets factors in regulating the spatial pattern of *Egfl7* in mouse (Wang et al., 2008).

Our finding that EGFL7 and miR-126 are both regulated in a CASZ1-dependent manner in humans is congruent with reports in mouse. However, despite complete conservation of miR-126 across species, we also demonstrate miR-126 has undergone an evolutionarily divergent and unique means of regulation exemplified by our findings that *Xenopus* miR-126 is expressed in domains mutually exclusive to *Egfl7* (i.e. somites) and expression of *Xenopus* miR-126 in the vasculature is CASZ1-independent. These observations are broadly consistent with recent reports that miR-126 transcription can occur independently of host gene transcription through differential intronic promoters (Monteys et al., 2010).

Conclusions

The vascular system arises via concerted efforts of individual ECs to harness their unique behaviors to assemble into tubular structures. The molecular and cellular mechanisms by which the vasculature arises are still unclear but we have identified previously unknown roles for CASZ1 in regulating sprouting and morphogenesis. While endothelium becomes stabilized and quiescent after embryonic development, vessels retain sensitivity to changes in environment due to injury, inflammation, or improper cardiac output thus making them susceptible to vascular dysfunction. In this regard, it is interesting that human CASZ1 has been linked to adult vascular diseases such as hypertension (Takeuchi et al., 2010). Events resulting in vascular dysfunction during this disease are associated with aberrant ECM remodeling, proliferation, and adhesion, all of which we have demonstrated to also be dysregulated upon depletion of CASZ1 (Lemarie et al., 2010). Therefore it will be intriguing to examine mechanisms by which CASZ1 itself is regulated and identify additional transcriptional targets that could trigger development of innovative therapeutic strategies in cardiovascular disease.

Experimental Procedures

Xenopus Embryo Collection and Morpholino Design

Preparation and collection of *Xenopus* embryos was performed as described (Showell et al., 2006). Embryos were staged according to Nieuwkoop and Faber (Nieuwkoop and Faber, 1967). MOs were obtained from Gene Tools, LLC. *Casz1*-specific MOs used as reported (Christine and Conlon, 2008). *Egfl7*-specific MO designed against acceptor region of *X. laevis* exon 6 and miR-126-specific MO designed against guide dicer region of *X. laevis* (Supplemental information).

In Situ Hybridization

Whole mount *in situ* analysis was carried out as described (Harland, 1991) using probes of *Casz1* (Christine and Conlon, 2008), *Msr* (Devic, 1996), *Ami* (Inui and Asashima, 2006), *Erg* (cloned from st. 39 *X. laevis* cDNA), *Egfl7* (cloned from st. 33-38 *X. tropicalis* cDNA), and *EphrinB2* (cloned from st. 39 *X. laevis* cDNA). miR-126 locked nucleic acid probe from Exiqon (38523-05) and hybridization was performed according to manufacturer's instructions at 51°C.

Chromatin Immunoprecipitation (ChIP)

Four hundred cardiovascular-enriched regions were dissected from st. 29 *X. tropicalis* embryos and processed for ChIP as reported (Weinmann and Farnham, 2002) (Taranova et

al., 2006) with following exceptions: (1)Sonication was carried out with Branson Digital Sonifier at 20% amplitude (2.5 cycles, 30s [1s on/0.5s off]) to yield 4kb DNA fragments. (2)Affinity-purified rabbit anti-CASZ1 polyclonal antibody was added and incubated overnight at 4°C. (3)DNA was digested with *NlaIII* (NEB) and ligated into *SphI*-digested (NEB) pUC19 using DNA ligation kit (Stratagene). Ligated DNA was transformed into NEB10β electrocompetent cells. Transformants were selected by blue/white screening, cultured, and isolated plasmids were sequenced. CASZ1 target DNA sequences were assessed by BLAT analysis using UCSC *X. tropicalis* Genome Browser (http://genome.ucsc.edu, August 2005 assembly). DNA scaffold location coordinates were imported into the annotated Joint Genome Institute. v4.1 database (http://genome.jgi-psf.org/Xentr4/Xentr4.home.html). Validation of targets by ChIP PCR was performed as above with following exceptions: (1)Thirty st. 32 *X. tropicalis* embryos were collected and processed as described. (2)Nuclear samples were sonicated at 20% amplitude (5 cycles, 30s [1s on/0.5s off]) to generate ~300bp DNA fragments.

In vivo Transcriptional Assays

Egfl7 intronic regions (introns 2,3,4,5) were subcloned into pGL3-Promoter firefly luciferase vector (Promega). *X. laevis* embryos were injected at 1-cell stage with 300 pg reporter plasmid and 10 pg Renilla reporter plasmid in presence or absence of CASZ1 mRNA. Injected embryos were cultured until st. 11.5. Ten injected embryos were lysed in 50 μl Passive Lysis Buffer (Promega) in triplicate. 20 μl of cleared lysates were assayed using Dual-Luciferase Reporter Assay System (Promega).

Cell Culture

Pooled population of HUVEC (Lonza) were maintained in Complete EBM-2 (Lonza) containing 10% fetal bovine serum, 100 U/mL penicillin and streptomycin and used between passages 1-6. hCASZ1 was IP'ed from HUVECs using polyclonal rabbit anti-human CASZ1 (LifeSpan Biosciences) and probed by western blot with same antibody.

shRNA

shRNA viral constructs specific to human *Casz1* and *Egfl7* were obtained from Open Biosystems TRC1 shRNA library. *Casz1, Egfl7*, and control scrambled sequence (Addgene) shRNA lentiviral particles were prepared by UNC Lentiviral Core Facility. 40-50% confluent HUVECs were infected with 1×10^6 IU lentivirus combined with 10 μg/mL polybrene (Sigma) for 7.5 hr. Infected cells were placed under 1.5 μg/mL puromycin selection for 3 days and processed for further analysis.

Live Time-Lapse Imaging

Cells seeded on uncoated or Fibronectin-coated (10 μg/mL) 12-well dishes, or embedded in fibrin gel were imaged over 24 hr using Olympus IX70 inverted microscope encased in Plexiglas housing to control internal environment (37°C, 5% CO_2 and relative humidity of 60%). Images were collected by Volocity 5.4.1 software.

Immunofluorescence

Cells seeded in chamber slides (BD Falcon) were fixed with cold methanol/acetone, blocked, and incubated with phospho-histone H3 (Millipore) or cleaved caspase-3 (Cell Signaling) overnight. Cells were incubated with rabbit anti-Cy3 (Sigma), stained with DAPI, and mounted (DakoCytomation). For cytoskeletal staining, cells were serum-starved (EBM-2+0.75% FBS) overnight, half of the cells were treated with 10μM Y-27632 (Sigma). Cells were fixed in 4% PFA, permeabilized with 0.1% Triton X-100, and incubated overnight with anti-vinculin (Sigma), and anti-phospho-paxillin (pY118, Invitrogen). Cells

were incubated with fluorescent secondary antibodies, stained with FITC-conjugated phalloidin (Invitrogen) and DAPI, mounted and imaged (Zeiss 710 or 700 microscope).

Sprouting Angiogenesis Assay

Sprouting assays were performed as described (Nakatsu et al., 2003; Sweet et al., 2012). Cells were stained with phalloidin (FITC) to visualize actin and with DRAQ5 to mark EC nuclei, and imaged (Olympus FLV500 inverted confocal microscope, 20× objective). Assay quantified measuring total length of protruding sprouts and number of branch points.

Western Blotting

Western blots were performed with 50 μg protein using RhoA (Santa Cruz), phosphomyosin light chain 2 (Cell Signaling [Ser 19]), RhoC (Santa Cruz [K-12]).

Statistical Analysis

Data are expressed as means ± SEM as indicated. Statistical analysis was done by Student's *t*-test and $p<0.05$ was considered significant.

Supplementary Material

Refer to Web version on PubMed Central for supplementary material.

Acknowledgments

This work is supported by grants to F.L.C from NIH/NHLBI (RO1 DE018825 and RO1 HL089641). N.M.A and K.S.C were supported by AHA awards. We are extremely grateful to faculty of Microscopy Services Lab at UNC for microscopy help and also John Wallingford, Mark Peifer, and Keith Burridge for helpful discussions and critical reading of manuscript.

References

Baltzinger M, Mager-Heckel AM, Remy P. Xl erg: expression pattern and overexpression during development plead for a role in endothelial cell differentiation. Dev Dyn. 1999; 216:420–433. [PubMed: 10633861]

Barton K, Muthusamy N, Fischer C, Ting CN, Walunas TL, Lanier LL, Leiden JM. The Ets-1 transcription factor is required for the development of natural killer cells in mice. Immunity. 1998; 9:555–563. [PubMed: 9806641]

Baudino TA, McKay C, Pendeville-Samain H, Nilsson JA, Maclean KH, White EL, Davis AC, Ihle JN, Cleveland JL. c-Myc is essential for vasculogenesis and angiogenesis during development and tumor progression. Genes Dev. 2002; 16:2530–2543. [PubMed: 12368264]

Bayless KJ, Davis GE. The Cdc42 and Rac1 GTPases are required for capillary lumen formation in three-dimensional extracellular matrices. J Cell Sci. 2002; 115:1123–1136. [PubMed: 11884513]

Burridge K, Wennerberg K. Rho and Rac take center stage. Cell. 2004; 116:167–179. [PubMed: 14744429]

Campagnolo L, Leahy A, Chitnis S, Koschnick S, Fitch MJ, Fallon JT, Loskutoff D, Taubman MB, Stuhlmann H. EGFL7 is a chemoattractant for endothelial cells and is up-regulated in angiogenesis and arterial injury. Am J Pathol. 2005; 167:275–284. [PubMed: 15972971]

Carmeliet P. Angiogenesis in health and disease. Nat Med. 2003; 9:653–660. [PubMed: 12778163]

Carmeliet P, Jain RK. Molecular mechanisms and clinical applications of angiogenesis. Nature. 2011; 473:298–307. [PubMed: 21593862]

Chan CH, Lee SW, Li CF, Wang J, Yang WL, Wu CY, Wu J, Nakayama KI, Kang HY, Huang HY, et al. Deciphering the transcriptional complex critical for RhoA gene expression and cancer metastasis. Nat Cell Biol. 2010; 12:457–467. [PubMed: 20383141]

Christine KS, Conlon FL. Vertebrate CASTOR is required for differentiation of cardiac precursor cells at the ventral midline. Dev Cell. 2008; 14:616–623. [PubMed: 18410736]

Chrzanowska-Wodnicka M, Burridge K. Rho-stimulated contractility drives the formation of stress fibers and focal adhesions. J Cell Biol. 1996; 133:1403–1415. [PubMed: 8682874]

Cleaver O, Tonissen KF, Saha MS, Krieg PA. Neovascularization of the Xenopus embryo. Dev Dyn. 1997; 210:66–77. [PubMed: 9286596]

Cox CM, D'Agostino SL, Miller MK, Heimark RL, Krieg PA. Apelin, the ligand for the endothelial G-protein-coupled receptor, APJ, is a potent angiogenic factor required for normal vascular development of the frog embryo. Dev Biol. 2006; 296:177–189. [PubMed: 16750822]

Davis GE, Koh W, Stratman AN. Mechanisms controlling human endothelial lumen formation and tube assembly in three-dimensional extracellular matrices. Birth Defects Res C Embryo Today. 2007; 81:270–285. [PubMed: 18228260]

De Val S. Key transcriptional regulators of early vascular development. Arterioscler Thromb Vasc Biol. 2011; 31:1469–1475. [PubMed: 21677289]

De Val S, Black BL. Transcriptional control of endothelial cell development. Dev Cell. 2009; 16:180–195. [PubMed: 19217421]

Devic E, Paquereau L, Vernier P, Knibiehler B, Audigier Y. Expression of a new G protein-coupled receptor X-msr is associated with an endothelial lineage in *Xenopus laevis*. Mechanisms of Development. 1996; 59:129–140. [PubMed: 8951791]

Fish JE, Santoro MM, Morton SU, Yu S, Yeh RF, Wythe JD, Ivey KN, Bruneau BG, Stainier DY, Srivastava D. miR-126 regulates angiogenic signaling and vascular integrity. Dev Cell. 2008; 15:272–284. [PubMed: 18694566]

Fitch MJ, Campagnolo L, Kuhnert F, Stuhlmann H. Egfl7, a novel epidermal growth factor-domain gene expressed in endothelial cells. Dev Dyn. 2004; 230:316–324. [PubMed: 15162510]

Harland RM. In situ hybridization: an improved whole mount method for Xenopus embryos. Meth Cell Biol. 1991; 36:675–685.

Inui M, Asashima M. A novel gene, Ami is expressed in vascular tissue in Xenopus laevis. Gene Expr Patterns. 2006; 6:613–619. [PubMed: 16431163]

Katoh K, Kano Y, Noda Y. Rho-associated kinase-dependent contraction of stress fibres and the organization of focal adhesions. J R Soc Interface. 2011; 8:305–311. [PubMed: 20826475]

Kokai E, Voss F, Fleischer F, Kempe S, Marinkovic D, Wolburg H, Leithauser F, Schmidt V, Deutsch U, Wirth T. Myc regulates embryonic vascular permeability and remodeling. Circ Res. 2009; 104:1151–1159. [PubMed: 19407242]

Kuhnert F, Mancuso MR, Hampton J, Stankunas K, Asano T, Chen CZ, Kuo CJ. Attribution of vascular phenotypes of the murine Egfl7 locus to the microRNA miR-126. Development. 2008; 135:3989–3993. [PubMed: 18987025]

Lelievre E, Hinek A, Lupu F, Buquet C, Soncin F, Mattot V. VE-statin/egfl7 regulates vascular elastogenesis by interacting with lysyl oxidases. EMBO J. 2008; 27:1658–1670. [PubMed: 18497746]

Lelievre E, Lionneton F, Soncin F, Vandenbunder B. The Ets family contains transcriptional activators and repressors involved in angiogenesis. Int J Biochem Cell Biol. 2001; 33:391–407. [PubMed: 11312108]

Lemarie CA, Tharaux PL, Lehoux S. Extracellular matrix alterations in hypertensive vascular remodeling. J Mol Cell Cardiol. 2010; 48:433–439. [PubMed: 19837080]

Levine AJ, Munoz-Sanjuan I, Bell E, North AJ, Brivanlou AH. Fluorescent labeling of endothelial cells allows in vivo, continuous characterization of the vascular development of Xenopus laevis. Dev Biol. 2003; 254:50–67. [PubMed: 12606281]

Levy D, Ehret GB, Rice K, Verwoert GC, Launer LJ, Dehghan A, Glazer NL, Morrison AC, Johnson AD, Aspelund T, et al. Genome-wide association study of blood pressure and hypertension. Nat Genet. 2009; 41:677–687. [PubMed: 19430479]

Mandel EM, Kaltenbrun E, Callis TE, Zeng XX, Marques SR, Yelon D, Wang DZ, Conlon FL. The BMP pathway acts to directly regulate Tbx20 in the developing heart. Development. 2010; 137:1919–1929. [PubMed: 20460370]

Monteys AM, Spengler RM, Wan J, Tecedor L, Lennox KA, Xing Y, Davidson BL. Structure and activity of putative intronic miRNA promoters. RNA. 2010; 16:495–505. [PubMed: 20075166]

Nakatsu MN, Sainson RC, Aoto JN, Taylor KL, Aitkenhead M, Perez-del-Pulgar S, Carpenter PM, Hughes CC. Angiogenic sprouting and capillary lumen formation modeled by human umbilical vein endothelial cells (HUVEC) in fibrin gels: the role of fibroblasts and Angiopoietin-1. Microvasc Res. 2003; 66:102–112. [PubMed: 12935768]

Narumiya S, Ishizaki T, Ufhata M. Use and properties of ROCK-specific inhibitor Y-27632. Methods in Enzymology. 2000; 325:273–284. [PubMed: 11036610]

Nichol D, Shawber C, Fitch MJ, Bambino K, Sharma A, Kitajewski J, Stuhlmann H. Impaired angiogenesis and altered Notch signaling in mice overexpressing endothelial Egfl7. Blood. 2010; 116:6133–6143. [PubMed: 20947685]

Nieuwkoop, PD.; Faber, J. Normal Table of *Xenopus laevis* (Daudin). Amsterdam, North Holland: 1967.

Nikolic I, Plate KH, Schmidt MH. EGFL7 meets miRNA-126: an angiogenesis alliance. J Angiogenes Res. 2010; 2:9. [PubMed: 20529320]

Nobes CD, Hall A. Rho, rac, and cdc42 GTPases regulate the assembly of multimolecular focal complexes associated with actin stress fibers, lamellipodia, and filopodia. Cell. 1995; 81:53–62. [PubMed: 7536630]

Parker LH, Schmidt M, Jin SW, Gray AM, Beis D, Pham T, Frantz G, Palmieri S, Hillan K, Stainier DY, et al. The endothelial-cell-derived secreted factor Egfl7 regulates vascular tube formation. Nature. 2004; 428:754–758. [PubMed: 15085134]

Parsons JT, Horwitz AR, Schwartz MA. Cell adhesion: integrating cytoskeletal dynamics and cellular tension. Nat Rev Mol Cell Biol. 2010; 11:633–643. [PubMed: 20729930]

Patan S. Vasculogenesis and angiogenesis as mechanisms of vascular network formation, growth and remodeling. J Neurooncol. 2000; 50:1–15. [PubMed: 11245270]

Potente M, Gerhardt H, Carmeliet P. Basic and therapeutic aspects of angiogenesis. Cell. 2011; 146:873–887. [PubMed: 21925313]

Rodrigues CO, Nerlick ST, White EL, Cleveland JL, King ML. A Myc-Slug (Snail2)/Twist regulatory circuit directs vascular development. Development. 2008; 135:1903–1911. [PubMed: 18469221]

Schmidt MH, Bicker F, Nikolic I, Meister J, Babuke T, Picuric S, Muller-Esterl W, Plate KH, Dikic I. Epidermal growth factor-like domain 7 (EGFL7) modulates Notch signalling and affects neural stem cell renewal. Nat Cell Biol. 2009; 11:873–880. [PubMed: 19503073]

Showell C, Christine KS, Mandel EM, Conlon FL. Developmental expression patterns of Tbx1, Tbx2, Tbx5, and Tbx20 in Xenopus tropicalis. Dev Dyn. 2006; 235:1623–1630. [PubMed: 16477648]

Strilic B, Kucera T, Eglinger J, Hughes MR, McNagny KM, Tsukita S, Dejana E, Ferrara N, Lammert E. The molecular basis of vascular lumen formation in the developing mouse aorta. Dev Cell. 2009; 17:505–515. [PubMed: 19853564]

Sweet DT, Chen Z, Wiley DM, Bautch VL, Tzima E. The adaptor protein Shc integrates growth factor and ECM signaling during postnatal angiogenesis. Blood. 2012; 119:1946–1955. [PubMed: 22096252]

Takeuchi F, Isono M, Katsuya T, Yamamoto K, Yokota M, Sugiyama T, Nabika T, Fujioka A, Ohnaka K, Asano H, et al. Blood pressure and hypertension are associated with 7 loci in the Japanese population. Circulation. 2010; 121:2302–2309. [PubMed: 20479155]

Taranova OV, Magness ST, Fagan BM, Wu Y, Surzenko N, Hutton SR, Pevny LH. SOX2 is a dose-dependent regulator of retinal neural progenitor competence. Genes Dev. 2006; 20:1187–1202. [PubMed: 16651659]

Wang S, Aurora AB, Johnson BA, Qi X, McAnally J, Hill JA, Richardson JA, Bassel-Duby R, Olson EN. The endothelial-specific microRNA miR-126 governs vascular integrity and angiogenesis. Dev Cell. 2008; 15:261–271. [PubMed: 18694565]

Warkman AS, Zheng L, Qadir MA, Atkinson BG. Organization and developmental expression of an amphibian vascular smooth muscle alpha-actin gene. Dev Dyn. 2005; 233:1546–1553. [PubMed: 15965984]

Weinmann AS, Farnham PJ. Identification of unknown target genes of human transcription factors using chromatin immunoprecipitation. Methods. 2002; 26:37–47. [PubMed: 12054903]

Xu K, Sacharidou A, Fu S, Chong DC, Skaug B, Chen ZJ, Davis GE, Cleaver O. Blood Vessel Tubulogenesis Requires Rasip1 Regulation of GTPase Signaling. Dev Cell. 2011; 20:526–539. [PubMed: 21396893]

Frank conlonHighlights

- CASZ1 is a conserved transcription factor required for vascular patterning
- CASZ1 controls endothelial cell adhesion, contractility, and proliferation.
- This control is exerted through the regulation of target genes *Egfl7* and miR-126.
- RhoA functions downstream of CASZ1/EGFL7 to mediate endothelial cell behavior.

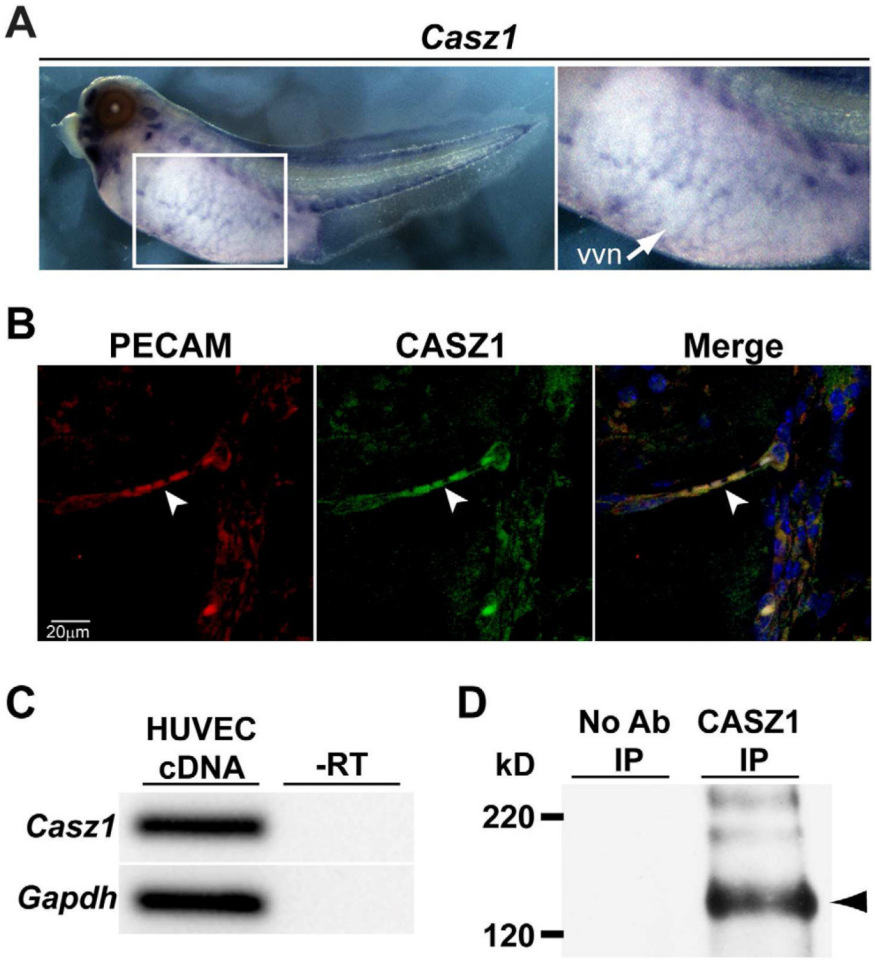

Figure 1. CASZ1 Expression in Vascular ECs is Evolutionarily Conserved

(A) *In situ* analysis of *Casz1 Xenopus* embryos (stage 41). Lateral view with anterior to left. *Casz1* is expressed in vascular structures including vitelline vein network (vvn, enlarged panel on right).

(B) CASZ1 (green) co-localizes with PECAM (red) in neural blood vessels of E14.5 mouse embryos.

(C) RT-PCR analysis of human *Casz1* in HUVEC cDNA. *Gapdh* was used as loading control.

(D) Immunoprecipitation (IP) of CASZ1 from HUVECs. Control lane (left) represents IP with no antibody (Ab). Arrowhead represents 125kD human CASZ1.

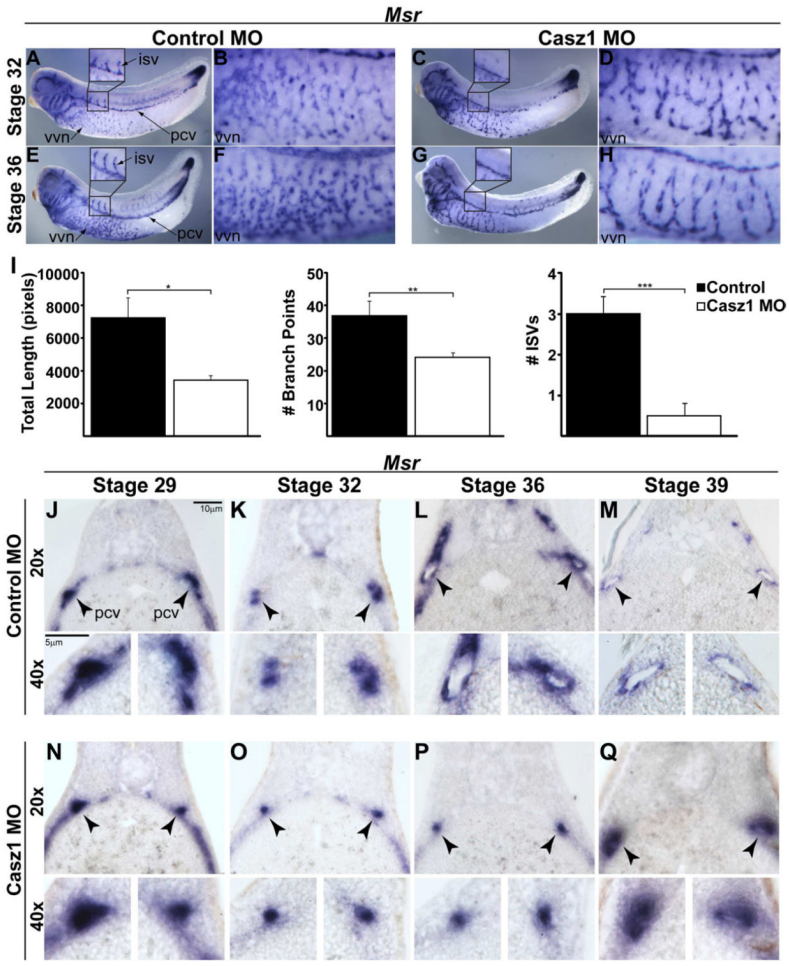

Figure 2. CASZ1 is Required for Vascular Development and Lumen Formation

(A-H) *In situ* analysis with EC marker *Msr* control and CASZ1-depleted embryos (stages 32-36; lateral view with anterior to left). Vessel patterning and branching within vitelline vein network (vvn) are severely compromised at stage 32 in CASZ1-depleted embryos (A,C high magnification of vvn in B,D) and stage 36 (E,G high magnification of vvn in F,H). Note poor sprouting of intersomitic vessels (isv) in CASZ1-depleted embryos at both stages (enlarged box in A,C,E,G). (n=10 embryos/condition/stage, 3 independent experiments).

(I) Quantification of vascular defects in control and CASZ1-depleted embryos (stage 36) representing combined total length of vessels, number of branch points within vvn, and number of isvs/embryo, respectively. Data represent mean ± SEM. (n=7 control and 10 Casz1 MO embryos). *: p<0.05; **:p<0.01; ***:p<0.001.

(J-Q) Histological analysis illustrates time course of lumen formation in *Xenopus* from stages 29-39 (J-M). Note posterior cardinal vein (pcv) lumens begin to open between stages 32 and 36 in control embryos (K,L) but fail to form in CASZ1-depleted embryos (N-Q). Dorsal is top, ventral is bottom. Arrowheads correspond to positions of pcv which are enlarged in lower panels (n=2-5 embryos/condition/stage). See also Figure S1.

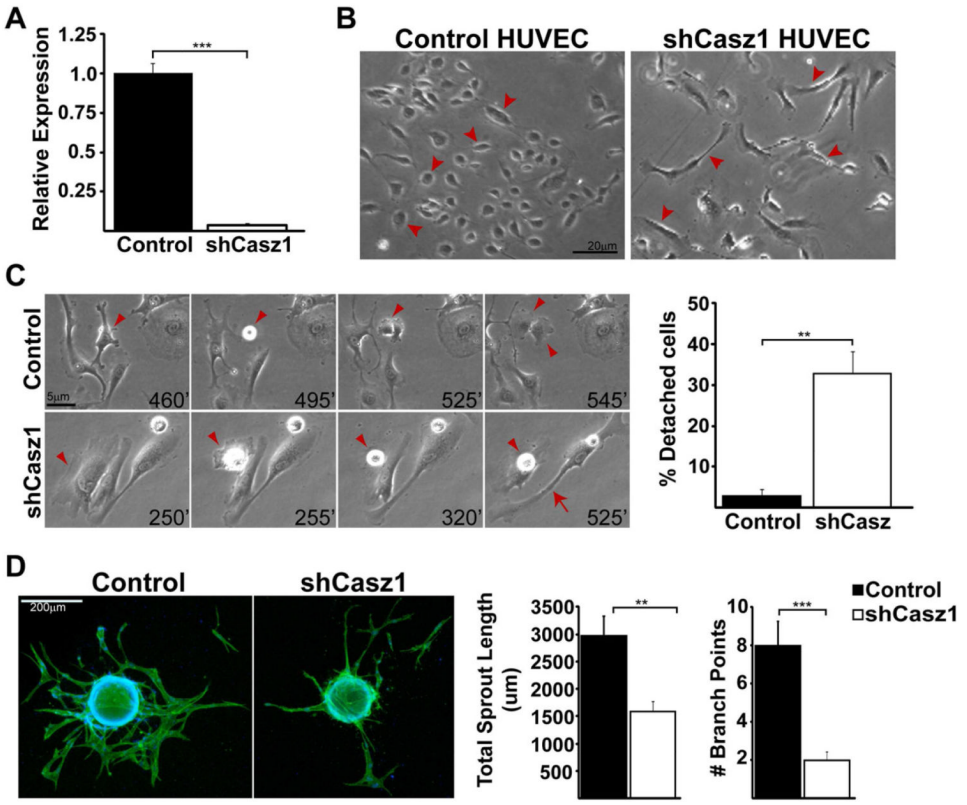

Figure 3. CASZ1 Regulates EC Behavior

(A) mRNA levels of *Casz1* after infection of HUVECs with shCasz1. *Casz1* is decreased by 16-fold. mRNA levels relative to *Rps29* ± SEM. ***: p<0.001.

(B) Phase contrast images of control and shCasz1 HUVECs. Controls display cobblestone-like morphology while CASZ1-depleted cells are thin and elongated (red arrowheads for examples of each).

(C) Time-lapse images of control and shCasz1 cells. Red arrowheads represent dividing control cell and rounded up CASZ1-depleted cell. Minutes elapsed presented at bottom right, taken every 5 min for 24 hr. Red arrow refers to elongated shCasz1 cell with trailing edge defects. Graph represents quantification of cells that round up and detach during imaging. Data represent mean ± SEM of 3 experiments conducted on independent batches of shRNA-infected cells (*n*=200 cells). **:p<0.01.

(D) Sprouting angiogenesis assay was performed with control and CASZ1-depleted HUVEC. On day 6, cultures were fixed and stained for phalloidin (green) and DRAQ5 (blue). Graphs represent mean ± SEM of total sprout length and number of branch points/bead (*n*=11 beads/condition). Experiments were repeated twice on independent batches of shRNA-infected cells. **:p<0.01; ***p<0.001. See also Figure S2, Movies S1 and S4.

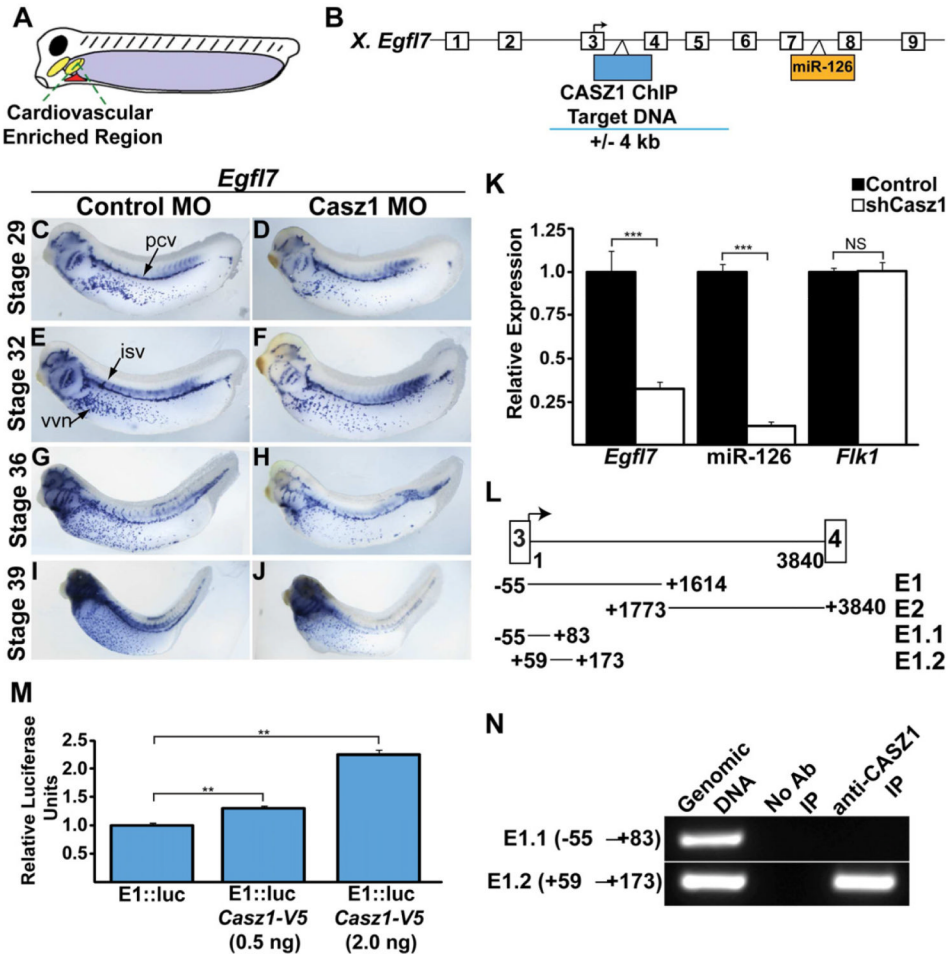

Figure 4. CASZ1 Directly Activates *Egfl7* Transcription

(A) Illustration of cardiovascular-enriched region dissected from *X. tropicalis* for chromatin immunoprecipitation (ChIP).

(B) Genomic structure of *Xenopus Egfl7* locus denoting CASZ1 ChIP fragment. White boxes: exons; shaded boxes, miR-126 in intron 7 and intronic region potentially containing CASZ1 element (+/- 4kb).

(C-J) *In situ* analysis of *Egfl7* of stages 29-39 control and CASZ1-depleted embryos (lateral view with anterior to left). Note downregulation of *Egfl7* in vitelline vein network (vvn) and intersomitic vessels (isv) in CASZ1-depleted embryos. Pcv-posterior cardinal vein.

(K) Relative mRNA expression of *Egfl7*, miR-126, and *Flk1* after infection of HUVECs with shCasz1. mRNA levels relative to *Rps29* ± SEM. ***:p<0.001; NS: not significant.

(L) Schematic demarcating *Egfl7* genomic DNA regions (in bp) tested for transcriptional activation. *E1* (-55–1614) within intron 3 but not *E2* (1773–3840) resulted in increased luciferase (luc) activity.

(M) *Egfl7* genomic region *E1* in presence or absence of *Casz1*. Bars represent fold increase in activity relative to control ± SEM. Experiments were repeated twice on independent batches of embryos, **:p<0.01.

(N) Identification of 90bp region endogenously bound by CASZ1located within non-overlapping region of *E1.2* (113-227) PCR amplicon. See also Figure S3.

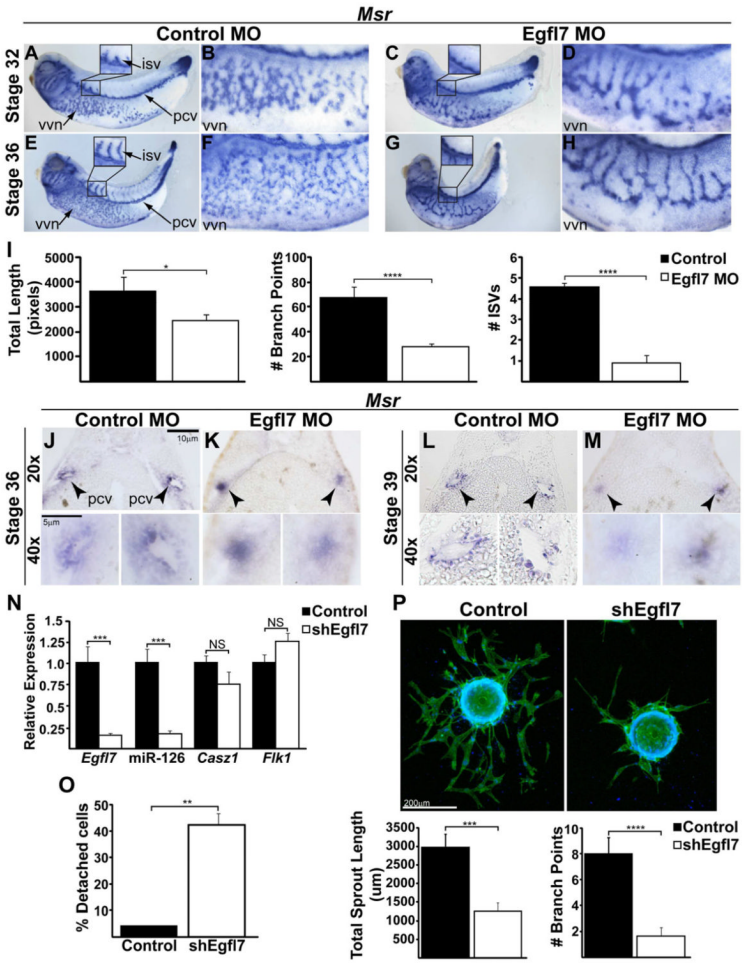

Figure 5. EGFL7-Depletion in Embryos and HUVECs Phenocopies CASZ1-Depletion

(A-H) *In situ* analysis with EC marker *Msr* control and EGFL7-depleted embryos (stages 32-36, lateral view with anterior to left). Note lack of branching in vitelline vein network (vvn) at stage 32 (A,C high magnification of vvn in B,D) and stage 36 (E,G high magnification of vvn in F,H). Intersomitic vessel (isv) sprouting is also impaired (A,C,E,G). (n=10 embryos/condition/stage, 3 independent experiments).

(I) Quantification of vascular defects control and EGFL7-depleted embryos (stage 36) representing total vessel length, number of branch points within vvn, and number of isvs/embryo. Data represent mean ± SEM. (n=7 control and 10 Egfl7 MO embryos). *:p<0.05; **:p<0.01; ****:p<0.0005.

(J-M) Histological analysis reveals lumenless posterior cardinal veins (pcv) in stage 36 (K) and stage 39 (M) Control and EGFL7-depleted embryos (J,L), dorsal top, ventral bottom, arrowheads correspond to pcv positions enlarged in lower panels (n=3 embryos/condition/stage).

(N) mRNA expression of *Egfl7*, miR-126, *Casz1, and Flk1* after infection of HUVECs with shEgfl7. *Egfl7* is decreased 11-fold. mRNA levels relative to *Rps29* ± SEM. ***:p<0.001; NS: not significant.

(O) Quantification of cells that round up and detach during imaging. Data represent mean ± SEM of 2 experiments conducted on independent batches of shRNA-infected cells. (n=100 cells). **:p<0.01.

(P) Sprouting angiogenesis assay was performed with control and EGFL7-depleted HUVEC. On day 6, cultures were fixed and stained for phalloidin (green) and DRAQ5 (blue). Graphs

represent mean ± SEM of total sprout length and number of branch points/bead (n=11 beads/condition). Experiments were repeated twice on independent batches of shRNA-infected cells. **:p<0.01; ***p<0.001. See also Figures S4-S5 and Movies S2 and S5.

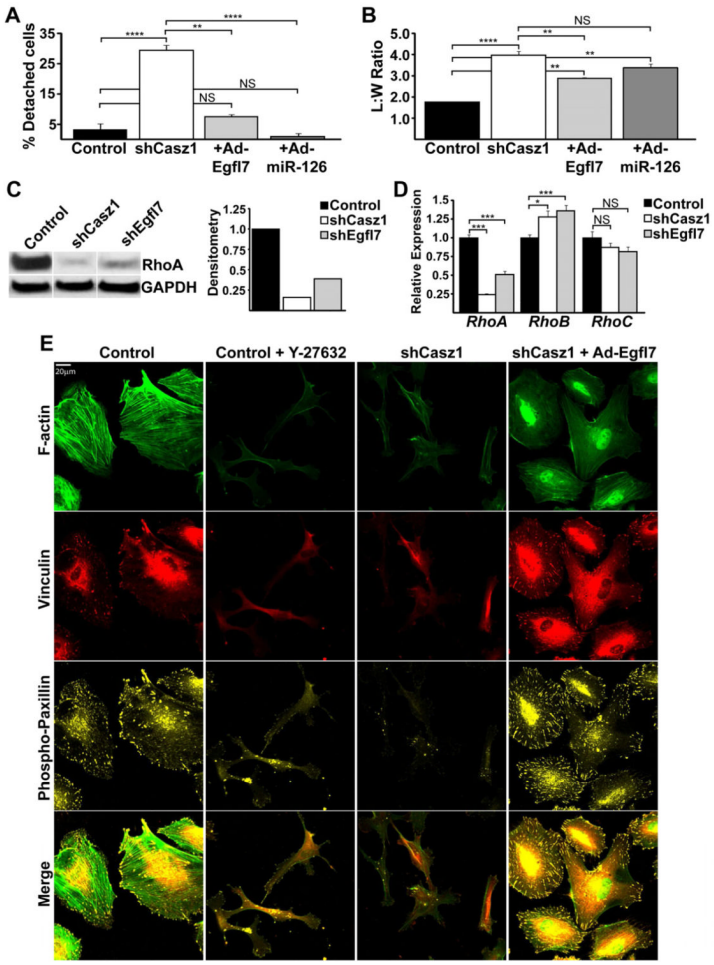

Figure 6. EGFL7 and miR-126 Play Distinct Roles Downstream of CASZ1

(A) Quantification of cells co-infected with shCasz1 and Ad-Egfl7 or Ad-miR-126 that round up and detach versus shCasz1 or control shRNA alone. Data represent mean ± SEM of 2 average experiments conducted on independent batches of shRNA-infected cells. (n=100 cells). **:p<0.01; ****:p<0.0005.

(B) Quantification of cell morphology determined by measuring length-to-width (L:W) ratio. Morphology was improved in cells co-infected with shCasz1 and Ad-Egfl7 but not in cells co-infected with Ad-miR-126. Data represent mean ± SEM of 3 experiments conducted on independent batches of shRNA-infected cells. (n=300-600 cells). **:p<0.01; ****:p<0.0005.

(C) RhoA protein expression in shRNA-infected HUVECs. RhoA levels were markedly decreased by depletion of CASZ1 and EGFL7. Graph of densitometry of RhoA levels relative to GAPDH.

(D) Relative *RhoA*, *RhoB*, and *RhoC* mRNA expression after shRNA infection. mRNA levels relative to *Rps29* ± SEM. *:p<0.05; ***:p<0.001; NS: not significant.

(E) Stress fibers and FAs disrupted in CASZ1-depleted HUVECs resemble cells treated with ROCK inhibitor Y-27632 (10μM). Restoration of *Egfl7* in CASZ1-depleted cells rescues proper FA localization. Phalloidin marks F-actin filaments (green), vinculin (red) and phosphorylated paxillin (yellow) mark FAs. See also Figure S6 and Movie S3.

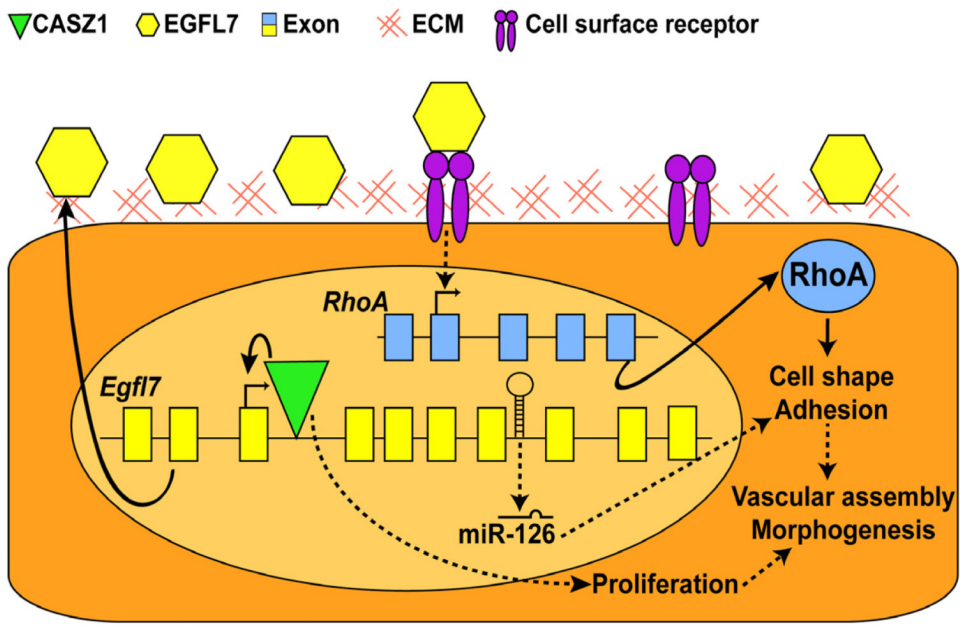

Figure 7. A model describing CASZ1 function in endothelial cells

CASZ1 functions by binding to an intronic element within the Egfl7 locus to activate proper levels of Egfl7 in endothelial cells. EGFL7 is then secreted to the extracellular matrix (ECM) where it likely binds cell-surface receptors which signal downstream to activate RhoA expression. Consequently, RhoA signaling modulates endothelial cell behaviors such as adhesion and contractility to promote vessel assembly and morphogenesis.